

## Energy Dependence of Two-Photon-Absorption Cross Sections in Anthracene

ITZCHAK WEBMAN AND JOSHUA JORTNER

*Department of Chemistry, Tel Aviv University, Tel Aviv, Israel*

(Received 26 September 1968)

Two-photon-absorption cross sections were determined in the energy range 3.10–3.56 eV for crystalline anthracene and for the anthracene molecule in solution. The experimental method was based on the measurement of the excitation spectrum for fluorescence induced by two-photon absorption from a Raman-shifted ruby laser. From these results we conclude that: (a) a symmetry-forbidden two-photon transition corresponding to the  ${}^1A_{1g} \rightarrow {}^1B_{2u}$  excitation was observed both in the crystal and in the solution; (b) this transition is vibronically induced by a nontotally symmetric vibration of the frequency  $1200 \pm 400 \text{ cm}^{-1}$ ; (c) a crystal state is observed at 3.5–3.6 eV which has no counterpart in the solution spectrum; (d) this crystal state is tentatively assigned to a *g*-symmetry-type charge-transfer state; (e) the possible observation of a quadrupole two-photon  ${}^1A_{1g} \rightarrow {}^1B_{2u}$  to the 0–0 band seems likely since the dipole two-photon transition is forbidden and vibronic mixing within the true 0–0 band does not occur.

## I. INTRODUCTION

Two-photon even-parity spectroscopy<sup>1–7</sup> is expected to provide new information concerning the energy levels of molecules and of solids, which may prove complementary to that obtained from the study of the conventional single-photon odd-parity spectroscopy. Two-photon spectroscopy provided interesting new data concerning even-parity Wannier exciton states and interband transitions in insulators such as the alkali halides,<sup>8–10</sup> CuCl,<sup>11</sup> CdS,<sup>12,13</sup> ZnS,<sup>14</sup> and TiCl.<sup>15,16</sup> On the other hand, our understanding of two-photon absorption in molecular crystal of aromatic molecules<sup>17–27</sup> is

yet far from being satisfactory. The lower excited states of these systems are reasonably well described within the framework of the tight-binding Frenkel exciton model,<sup>28</sup> which rests on the assumption that the crystal states have a unique parentage in the molecular states. Two recent extensions of the Frenkel model for molecular crystals of organic molecules have to be considered in this context:

(a) Choi *et al.*<sup>29</sup> discussed charge-transfer states, where an electron is removed from one molecule and located on another, so that the excitation wave corresponds to the coherent motion of the center of mass of the electron and the associated hole. The location of these charge-transfer states is as yet somewhat uncertain. Estimates based on a semiclassical model led to the energy of  $3.4 \pm 0.5 \text{ eV}$  in anthracene.<sup>29</sup> The photoemission data of Pope and Burgos<sup>30</sup> were interpreted in terms of a charge-transfer state located at 3.45 eV in crystalline anthracene.

(b) Metastable exciton states above the direct threshold to the conduction band, which in crystalline anthracene is located at 4.1 eV,<sup>31,32</sup> should be treated by the Fano configuration-interaction scheme,<sup>33–35</sup> which in this case involves one closed channel (the Frenkel state) decaying into two open channels, which involve radiationless intramolecular decay<sup>35</sup> and autoionization.<sup>34</sup>

Crystalline anthracene has proved to be of special interest in view of the extensive information available from one-photon odd-parity spectroscopy and from theoretical calculations of the exciton band structure in

<sup>1</sup> M. Goepfert-Mayer, *Ann. Physik* **9**, 273 (1931).<sup>2</sup> R. Braustein, *Phys. Rev.* **125**, 475 (1962).<sup>3</sup> D. A. Kleinman, *Phys. Rev.* **125**, 87 (1962).<sup>4</sup> R. Loudon, *Proc. Phys. Soc. (London)* **80**, 952 (1962).<sup>5</sup> R. Braustein and N. Ockman, *Phys. Rev.* **134**, A499 (1964).<sup>6</sup> A. Gold and J. P. Hernandez, *Phys. Rev.* **139**, A2002 (1965).<sup>7</sup> M. Inoue and Y. Toyozawa, *J. Phys. Soc. Japan* **20**, 363 (1965).<sup>8</sup> J. J. Hopfield and J. M. Worlock, *Phys. Rev.* **137**, A1455 (1965).<sup>9</sup> J. J. Hopfield, J. M. Worlock, and K. Park, *Phys. Rev. Letters* **11**, 414 (1963).<sup>10</sup> D. Fröhlich and B. Stagginnus, *Phys. Rev. Letters* **19**, 496 (1967).<sup>11</sup> D. Fröhlich, B. Stagginnus, and E. Shonherr, *Phys. Rev. Letters* **19**, 1032 (1967).<sup>12</sup> P. J. Regensburger and E. Panniza, *Phys. Rev. Letters* **18**, 113 (1967).<sup>13</sup> V. K. Koniukhlov, L. A. Kulevskii, and M. A. Prokhnov, *Phys. Status Solidi* **21**, K107 (1967).<sup>14</sup> E. Panniza, *Appl. Phys. Letters* **10**, 265 (1967).<sup>15</sup> M. Matsuoka and T. Yajima, *J. Phys. Soc. Japan* **23**, 1028 (1967).<sup>16</sup> M. Matsuoka and T. Yajima, *Phys. Letters* **23**, 54 (1966).<sup>17</sup> W. L. Peticolas, J. P. Goldsborough, and K. E. Rieckhoff, *Phys. Rev. Letters* **10**, 43 (1963).<sup>18</sup> W. L. Peticolas and K. E. Rieckhoff, *J. Chem. Phys.* **39**, 1347 (1963).<sup>19</sup> S. Singh and B. P. Stoicheff, *J. Chem. Phys.* **38**, 2032 (1963).<sup>20</sup> S. Singh, W. J. Jones, W. Siebrand, R. P. Stoicheff, and W. G. Schneider, *J. Chem. Phys.* **42**, 330 (1965).<sup>21</sup> J. L. Hall, P. A. Jennings, and R. M. McClintock, *Phys. Rev. Letters* **11**, 364 (1963).<sup>22</sup> A. Bergman, M. Levine, and J. Jortner, *Phys. Rev. Letters* **18**, 593 (1966).<sup>23</sup> D. Fröhlich and H. Mahr, *Phys. Rev. Letters* **18**, 593 (1966).<sup>24</sup> F. C. Strome, Jr., *Phys. Rev. Letters* **20**, 3 (1968).<sup>25</sup> D. H. McMahon, R. A. Soref, and A. R. Franklin, *Phys. Rev. Letters* **14**, 1060 (1965).<sup>26</sup> M. D. Galanin and Z. A. Chizikova, *JETP Letters* **4**, 27 (1966).<sup>27</sup> J. P. Hernandez and A. Gold, *Phys. Rev.* **156**, 26 (1967).<sup>28</sup> See, for example, A. S. Davydov, *Sov. Phys.—Usp.* **82**, 145 (1964).<sup>29</sup> S. I. Choi, J. Jortner, S. A. Rice, and R. Silbey, *J. Chem. Phys.* **41**, 3294 (1964).<sup>30</sup> M. Pope and J. Burgos, *Mol. Cryst.* **1**, 395 (1966).<sup>31</sup> G. Kastro and J. F. Hornig, *J. Chem. Phys.* **42**, 1459 (1965).<sup>32</sup> R. F. Chaiken and D. R. Kearns, *J. Chem. Phys.* **45**, 3966 (1966).<sup>33</sup> U. Fano, *Phys. Rev.* **124**, 1866 (1961).<sup>34</sup> S. I. Choi, *Phys. Rev. Letters* **19**, 358 (1967).<sup>35</sup> J. Jortner, *Phys. Rev. Letters* **20**, 244 (1968).

this system<sup>36</sup> which serves as a convenient model system for molecular crystals of aromatic molecules. New information on the crystal states will result from the understanding of the even-parity transitions. The available experimental information on two-photon spectroscopy in this system can be summarized as follows:

(a) The blue fluorescence<sup>18-21</sup> induced by two-photon absorption from a ruby laser ( $h\nu = 1.78$  eV) results from the radiative decay of the lowest vibronic components ( $Au$  and  $Bu$ ) of the  ${}^1B_{2u}$  exciton state. At moderately high-exciting light intensities, when singlet-singlet exciton annihilation is negligible,<sup>22</sup> the dependence of the fluorescence intensity  $F$  on the flux  $I$  of the exciting light is

$$F = \eta n V \sigma I^2, \quad (1)$$

where  $V$  is the irradiated volume,  $\eta$  is the quantum yield for emission,  $n$  is the number of molecules per unit volume, and  $\sigma$  corresponds to the two-photon absorption cross section per molecule (expressed in units of  $\text{cm}^4 \cdot \text{second photon}^{-1}$ ). The experimental value  $\sigma = (3 \pm 1) \times 10^{-61} \text{ cm}^4 \cdot \text{sec photon}^{-1}$  at  $2h\nu = 3.56$  eV was reported by several groups.<sup>18,21,22</sup>

(b) Two-photon-absorption cross sections at higher energies were recently measured by Strome<sup>24</sup> utilizing anti-Stokes Raman emission induced by a ruby laser. Fluorescence data, resulting from excitation in the energy range 4.0-4.7 eV led to the cross sections:

$$\sigma = 7.6 \times 10^{-50} \text{ cm}^4 \cdot \text{sec photon}^{-1} \quad \text{at } 2h\nu = 4.15 \text{ eV,}$$

$$\sigma = 3.7 \times 10^{-48} \text{ cm}^4 \cdot \text{sec photon}^{-1} \quad \text{at } 2h\nu = 4.3 \text{ eV,}$$

$$\sigma = 1.2 \times 10^{-48} \text{ cm}^4 \cdot \text{sec photon}^{-1} \quad \text{at } 2h\nu = 4.7 \text{ eV.}$$

(c) The energy dependence of the two-photon-absorption cross sections in the range 3.4-4.2 eV was reported by Fröhlich and Mahr<sup>28</sup> who utilized the two-beam method. Two states located at 3.48 and at 3.58 eV were observed in the crystal. Two-photon absorption below 3.45 eV was too weak to be detected by this experimental method.

(d) The relative two-photon-absorption cross sections for the anthracene crystal and for the isolated anthracene molecule in solution have been reported at  $2h\nu = 3.56$  eV from fluorescence studies. McMahan *et al.*<sup>25</sup> have reported the value

$$\sigma_{\text{crystal}} / \sigma_{\text{solution}} = 15$$

while Galanin and Chizikova<sup>26</sup> obtained

$$\sigma_{\text{crystal}} / \sigma_{\text{solution}} = 8$$

at this energy.

Since the pioneering experimental work of Singh and Stoicheff<sup>19</sup> and of Peticolas *et al.*,<sup>17</sup> a lively theoretical debate has followed concerning the nature of the 3.56-eV two-photon excited state in anthracene. The following interpretations were proposed:

(a)  $g$ -type molecular states: The first theoretical interpretations rested on the assumption that the  ${}^1A_{1g}$  or the  ${}^1B_{1g}$  molecular states of anthracene are located at 3.6 eV.<sup>17,19</sup> The Pariser-Parr molecular calculations (which are reliable for  $u$ -type states) indicate that the  $g$ -type states of the anthracene molecule should be located at appreciably higher energy, e.g., at about 5 eV.<sup>37</sup> Besides, the observed  $\sigma$  value at 3.6 eV seems to be too low for this assignment, as the cross section for an allowed two-photon transition to a  $g$ -type molecular state was estimated to be about  $10^{-48} \text{ cm}^4 \cdot \text{sec photon}^{-1}$  for typical aromatic molecules.<sup>38,39</sup>

(b)  $g$ -type crystal states: Hernandez and Gold<sup>27</sup> have suggested that the  ${}^1A_g$  and the  ${}^1B_g$  crystal exciton states originating from the molecular  ${}^1B_{1g}$  state are located around 3.7 eV. This  ${}^1B_{1g}$  state was assumed to be located at 4.94 eV in the free molecule,<sup>37</sup> and the dominating contribution to the level shift in the crystal was assumed to arise from the environmental shift.<sup>27</sup>

(c) Symmetry-forbidden two-photon transitions: Odd-parity two-photon transitions (e.g.,  $g \rightarrow u$  excitations) can be induced by vibronic coupling effects.<sup>6,20,38,40</sup> It was proposed that the transition at  $2h\nu = 3.56$  eV arises from the vibronic admixture of even parity  $A_g$  and  $B_g$  crystal states into the  $Au$  and  $Bu$  components of the  ${}^1B_{2u}$  state. It was later suggested by Albrecht<sup>41</sup> that the symmetry-forbidden transition to the  ${}^1B_{3u}$  state may be responsible for the two-photon absorption reported by Fröhlich and Mahr<sup>28</sup> in that region.

The questions which we attempt to answer in the present work are as follows:

(a) What physical information can be obtained concerning symmetry-forbidden two-photon transitions in the molecular crystal and in the corresponding isolated molecule?

(b) What is the relation between the two-photon-absorption spectrum of the isolated organic molecule and the molecular crystal? In the conventional case of odd-parity one-photon spectroscopy, the crystal effects are manifested by Davydov splittings, level shifts, and intensity changes enhanced by crystal field mixing. Similar effects will prevail for both even-parity and for symmetry-forbidden odd-parity two-photon transitions.

<sup>37</sup> R. Pariser, *J. Chem. Phys.* **24**, 250 (1956).

<sup>38</sup> E. M. Evleth and W. L. Peticolas, *J. Chem. Phys.* **41**, 1400 (1964).

<sup>39</sup> (a) B. Honig, J. Jortner, and A. Szoke, *J. Chem. Phys.* **46**, 2714 (1967); (b) B. Honig, B. Sharf, and J. Jortner (unpublished).

<sup>40</sup> W. L. Peticolas, M. W. Dowley, and K. B. Eisenthal, *J. Chem. Phys.* **47**, 1609 (1967).

<sup>41</sup> A. C. Albrecht, quoted in Ref. 23.

<sup>36</sup> See, for example, (a) A. Matsui and Y. Ishii, *J. Phys. Soc. Japan* **23**, 581 (1967); (b) S. A. Rice and J. Jortner, in *Physics and Chemistry of the Organic Solid State*, D. Fox, M. M. Labes, and A. Weissberger, Eds. (Interscience Publishers, Inc., New York, 1967), Vol. 3, p. 201.

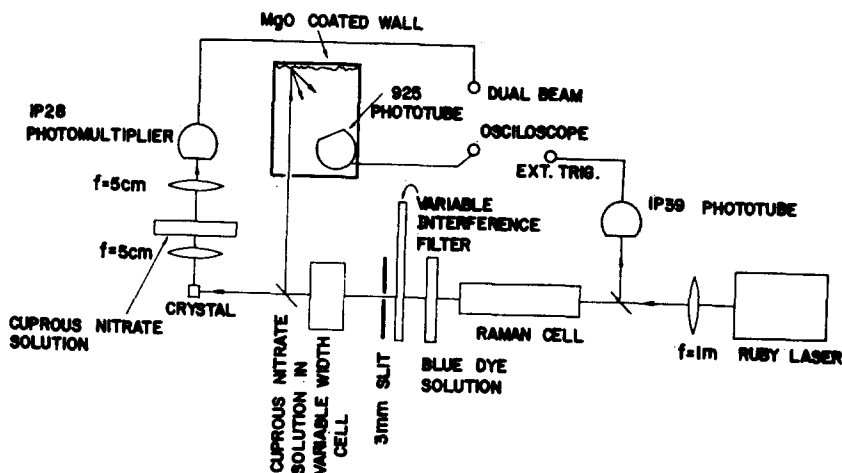


FIG. 1. A schematic diagram of the experimental arrangement.

(c) What evidence can be obtained from two-photon spectroscopy concerning crystal states which do not have a counterpart in the states of the isolated molecule, and cannot be described within the framework of the tight-binding Frenkel exciton model?

Two-photon spectroscopy can provide interesting information concerning the location of charge-transfer states in molecular crystals of aromatic molecules. Triplet and singlet  $u$ -type charge-transfer states were previously considered in some detail.<sup>29,42</sup> Unfortunately, singlet  $u$ -type charge-transfer states are expected to be characterized by a low oscillator strength in one-photon spectroscopy,<sup>43</sup> and in this case they will be obscured by the relatively strong transitions to the lower-lying  $u$ -type Frenkel exciton state. Now,  $g$ -type charge-transfer states can be easily constructed and their energetic shift from the corresponding charge-transfer  $u$  states is expected to be small. These  $g$ -type charge-transfer states may be amenable to experimental observation by two-photon spectroscopy. In this case the mapping of these even-parity states will be not necessarily masked by the lower  $u$ -type Frenkel exciton states, which are now only vibronically induced.

In the present work we report the results of an experimental study of the energy dependence of two-photon-absorption cross sections for crystalline anthracene and for the anthracene molecule in solution in the energy range  $2h\nu = 3.10\text{--}3.56$  eV. Experimental information or odd-parity vibronically-induced two-photon transitions is obtained, and evidence for a new crystal state in the range 3.5–3.6 eV is presented. These data combined with the previous results of Fröhlich and Mahr<sup>23</sup> and of Storme<sup>24</sup> provide a self-consistent semi-quantitative picture of the even-parity excited states of crystalline anthracene.

<sup>42</sup> R. Greer, S. A. Rice, J. Jortner, and R. Silbey, *J. Chem. Phys.* (unpublished).

<sup>43</sup> R. S. Berry, J. Jortner, J. C. Mackie, E. S. Pysh, and S. A. Rice, *J. Chem. Phys.* **42**, 1535 (1965).

## II. EXPERIMENTAL PROCEDURE

Reliable information on two-photon-absorption cross sections in anthracene can be obtained from the two-photon induced-fluorescence action spectrum because of the following reasons:

(a) The quantum yield for emission is high,  $\eta = 0.96 \pm 0.03$  in the crystal and  $\eta = 0.25\text{--}0.33$  in solution.<sup>44</sup>

(b) The fluorescence quantum yield is independent of the one-photon-excitation frequency in the range 3.0–4.5 eV,<sup>45</sup> and a similar situation is expected to prevail for two-photon excitation.

The experimental method utilized by us is based on the measurement of the excitation spectrum for fluorescence induced by two-photon absorption from a Raman-shifted ruby laser which provides a variety of secondary laser frequencies in the range 3.1–3.56 eV.<sup>46</sup> The obvious advantage of this technique over the "conventional" two-photon spectroscopy using the two-beam method<sup>8,23</sup> involves its high sensitivity which makes possible the determination of cross sections of the order of  $\sigma \gtrsim 10^{-64}$  cm<sup>4</sup>·sec photon<sup>-1</sup>. The main limitation of this method is due to the low spectral resolution which can be achieved.

A schematic diagram of the experimental arrangement is shown in Fig. 1. In order to provide high-intensity excitation sources in the range 12 000–14 400 cm<sup>-1</sup> we have used a Korad K1Q passively switched giant-pulsed ruby laser, emitting a pulse of 20-MW peak intensity in 20–25 nsec, as an excitation source for stimulated Raman emission in several organic liquids. The following liquids were employed for the generation of first and second Stokes radiation in the range between 1% and 15% of the ruby-laser intensity:

<sup>44</sup> See, for example, R. E. Kellog, *J. Chem. Phys.* **44**, 411 (1966).

<sup>45</sup> W. H. Melhuish, *J. Phys. Chem.* **65**, 229 (1961).

<sup>46</sup> G. Eckhardt, *J. Quantum Electron.* **2**, 1, 8 (1966). The use of a Raman-shifted ruby laser source to map out this region was suggested by Hall *et al.* (Ref. 21).

Tetrachloroethylene ( $2h\nu=27\,906$  and  $27\,012\text{ cm}^{-1}$ ), carbon disulfide ( $2h\nu=27\,488$  and  $26\,176\text{ cm}^{-1}$ ), orthoxylyene ( $2h\nu=27\,240$  and  $25\,880\text{ cm}^{-1}$ ), tetrachloroethylene ( $2h\nu=27\,012\text{ cm}^{-1}$ ), benzene ( $2h\nu=26\,820\text{ cm}^{-1}$ ), toluene ( $2h\nu=26\,792$  and  $24\,784\text{ cm}^{-1}$ ), nitrobenzene ( $2h\nu=26\,112\text{ cm}^{-1}$ ), and styrene ( $2h\nu=25\,542\text{ cm}^{-1}$ ). The laser beam was directed through a cell 60 cm long containing the Raman liquid and was slightly concentrated by a  $f=1\text{-m}$  lens. A light-filtering system placed behind the cell was used to pass only the required wavelength. This system consisted of a blue dye solution (cryptocyanine in methanol) which is characterized by a sharp cutoff at  $7100\text{ \AA}$ . The dye solution was made sufficiently concentrated to prevent its bleaching by the laser light. The dye cell was followed by a Jena Glaswerk variable-wavelength interference filter with a 3-mm slit centered at the appropriate wavelength. After being attenuated by the light-filtering system the peak intensities of the Raman sources ranged from 20–600 kW, i.e., peak fluxes of  $7\times 10^{22}$ – $2\times 10^{24}$  photons  $\text{sec}^{-1}$ . A part of the emerging (Raman-shifted) beam was reflected onto a ground-glass plate from which the light was collected into a Bausch and Lomb 500-mm grating monochromator adapted with a 925 S1 phototube. In this manner the Stokes emission was detected and the light-filtering system was checked. The intensity of the beam could be varied by attenuation when passed through a cuprous nitrate solution in a variable length cell (cell length 0.1–20 mm). The crystal was irradiated by an unfocused beam of a cross section of  $0.2\text{ cm}^2$ .

The system collecting the blue fluorescence light consisted of a  $f=5\text{-cm}$  lens, a 2-cm-wide cell of concentrated cuprous nitrate solution and a second  $f=5\text{-cm}$  lens refocusing the light on the S-1 cathode of an IP28 photomultiplier. Work in the linear range of the photomultiplier was achieved by attenuating the entering blue light by a neutral density filter and using two wide dynamic-range HP 460 BR amplifiers in cascade to preamplify the signal from the photomultiplier. The output was fed into a Tektronix 555 dual-beam oscilloscope, the other trace of which was used for the monitoring of the intensity of exciting light. For this purpose a fraction of the exciting light was directed through a hole into a light-tight compartment (replacing the monochromator described above) having a back wall coated with MgO. The scattered light was detected by a 925 S-1 diode mounted inside the compartment. The trace was recorded by a Polaroid camera using Polaroscope 410 high-speed film.

The high-purity zone-refined anthracene single crystal of dimensions  $7\times 10\times 10\text{ mm}$  was oriented in such a manner that the polarization of the exciting light was perpendicular to the cleavage plane. For each exciting wavelength measurements were performed both at the Stokes frequency and at the laser frequency. For the excitation at the laser frequency the blue

dye solution was exchanged by a dilute cuprous nitrate solution and the filter was realigned for  $6943\text{ \AA}$ . In this manner similar excitation conditions at the laser and the Stokes frequencies were provided.

For the measurements at liquid-nitrogen temperature ( $77^\circ\text{K}$ ) the crystal was attached to a cold finger of a cryostat equipped with a window for passing the exciting beam, and a wide window at a perpendicular direction for the collection of the fluorescent light.

A similar setup was used for the measurements of two-photon absorption of anthracene in benzene solution. In order to get higher exciting intensities we omitted the interference filter and the slit. The monitoring of the exciting beam was carried out through the Bausch and Lomb monochromator in order to check the spectral purity of the source. A  $0.09M$  solution of anthracene in benzene was used. The solution was contained in a  $1\times 1\text{ cm}$  cell. No concentration dependence of the two-photon-absorption cross sections was found. The ratio of cross section in the crystal to that of anthracene in solution was measured at  $28\,800\text{ cm}^{-1}$ . First the solution was excited by a 1-MW laser beam. The crystal was then excited using an equivalent geometry, with the intensity of the laser beam attenuated. The fluorescence detection geometries were the same in both cases.

### III. EXPERIMENTAL RESULTS

#### A. The Crystal Data

The measurements of the energy dependence of the two-photon-absorption cross sections involved the comparison of the  $\sigma$  value at the (Raman-shifted) energy  $2h\nu$  with the cross section at the (ruby-laser) energy  $2h\nu=28\,800\text{ cm}^{-1}$ . Plots of the dependence of peak fluorescence intensity on the peak excitation intensity are displayed in Fig. 2, and reveal the linear dependence of  $F$  on  $I^2$ , as expected for two-photon absorption. The absolute values of  $\sigma$  at various energies were computed by taking the value<sup>21,22</sup>  $\sigma=3\times 10^{-51}\text{ cm}^4\cdot\text{sec photon}^{-1}$  at  $2h\nu=28\,800\text{ cm}^{-1}$  which was previously also measured in this laboratory. These results are summarized in Fig. 3. The relative  $\sigma$  values are accurate within 25% while the absolute values are reliable only within about 50%. The following features of these crystal data should be noted:

(a) Very low  $\sigma$  values were observed in the range  $24\,800$ – $26\,000\text{ cm}^{-1}$  which corresponds to the 0–0 band of the one-photon absorption.

(b) The low-energy two-photon-absorption cross sections were measured both at room temperature and at liquid-nitrogen temperature. The values of the ratios  $\sigma_{28\,800}/\sigma_{25\,540}$  and  $\sigma_{28\,800}/\sigma_{24\,784}$  were found to be independent of temperature in the range  $300^\circ$ – $77^\circ\text{K}$  within an experimental error of 50%. We may

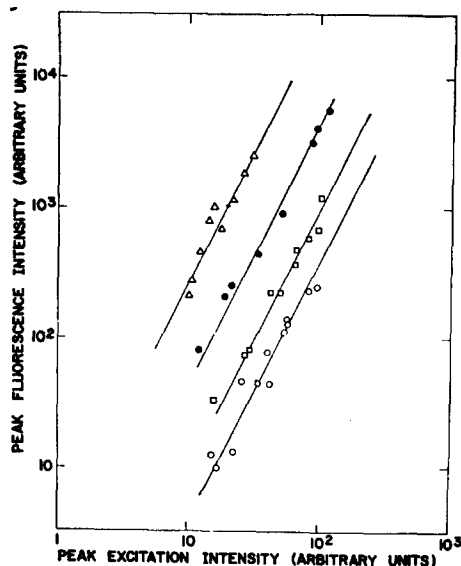


FIG. 2. The dependence of the two-photon-excited peak fluorescence intensity in crystalline anthracene on the peak excitation intensity.  $\Delta$   $2h\nu=28\,800\text{ cm}^{-1}$ ,  $\bullet$   $2h\nu=27\,340\text{ cm}^{-1}$ ,  $\square$   $2h\nu=25\,880\text{ cm}^{-1}$ ,  $\circ$   $2h\nu=25\,542\text{ cm}^{-1}$ . These results correspond to measurements at room temperature. All the  $F$  and  $I$  data are displayed on the same arbitrary scale.

thus conclude that the major contribution to the weak two-photon absorption in the range  $24\,800\text{--}26\,000\text{ cm}^{-1}$  does not arise from hot bands.

(c) In the range  $25\,900\text{--}26\,800\text{ cm}^{-1}$  an increase of the values with increasing energy is observed.

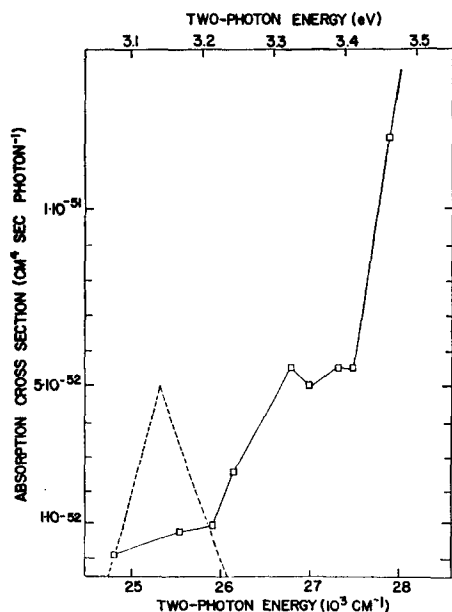


FIG. 3. The energy dependence of two-photon-absorption cross sections in crystalline anthracene. The value  $\sigma=3\times 10^{-51}\text{ cm}^2\cdot\text{sec photon}^{-1}$  at  $2h\nu=28\,800\text{ cm}^{-1}$  was not included on this linear scale. The dashed triangle represents the unpolarized one-photon  $^1A_{1g}\rightarrow^1B_{2u}$  0-0 transition in the crystal (see Ref. 36).

(d) In the region  $26\,750\text{--}27\,500\text{ cm}^{-1}$  we have measured values at a spacing of  $200\text{--}300\text{ cm}^{-1}$ . These values lie in the range  $\sim 5\times 10^{-52}\text{ cm}^2\cdot\text{sec photon}^{-1}$ , i.e., about 20% of the value at  $28\,800\text{ cm}^{-1}$ . A decrease of the  $\sigma$  values towards lower energy starts in the region  $26\,400\text{--}26\,750\text{ cm}^{-1}$ .

(e) The low  $\sigma$  values in the region up to  $27\,500\text{ cm}^{-1}$  ( $3.4\text{ eV}$ ) are consistent with the negative results of Fröhlich and Mahr.<sup>23</sup>

(f) A sharp increase of the  $\sigma$  values is observed at the energy range above  $27\,500\text{ cm}^{-1}$ . The value  $\sigma=1.2\times 10^{-51}\text{ cm}^2\cdot\text{sec photon}^{-1}$  measured by us at  $2h\nu=27\,906$

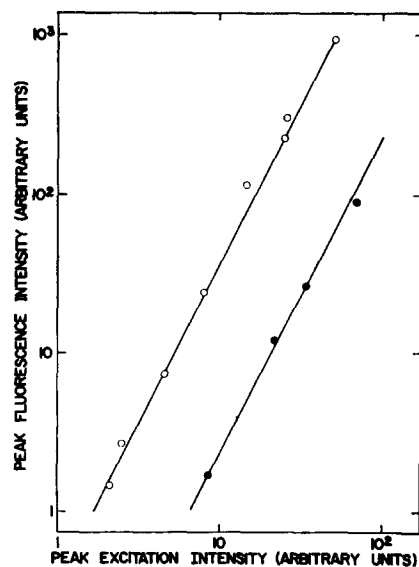


FIG. 4. The dependence of the peak fluorescence intensity against the peak excitation intensity for the crystal (open circles) and for the solution (solid circles) at  $2h\nu=28\,800\text{ cm}^{-1}$ . The scale for the  $F$  values is the same for both cases. The scale for the  $I$  values is lower by a factor of 30 for the crystal data than for the solution data.

$\text{cm}^{-1}$  is consistent with the results of Fröhlich and Mahr.<sup>23</sup> As already pointed out by these authors<sup>23</sup> the  $\sigma$  value used by us at  $2h\nu=28\,800\text{ cm}^{-1}$  is also consistent with their results.

(g) The  $\sigma$  value at  $2h\nu=28\,800\text{ cm}^{-1}$  was found to be temperature-independent in the range  $300^\circ\text{--}77^\circ\text{K}$  in agreement with the data of Singh *et al.*<sup>20</sup>

### B. Comparison of the Cross Section in the Crystal and in Solution

The  $\sigma$  values for crystalline anthracene and for anthracene in benzene solution were compared at  $2h\nu=28\,800\text{ cm}^{-1}$ . The plots of  $F$  vs  $I$  obtained under equivalent excitation and detection conditions are presented in Fig. 4. Taking into account the difference in the quantum yields for the fluorescence emission from the crystal solution  $\eta_{\text{crystal}}/\eta_{\text{solution}}=3$  we obtain from Eq.

(1)  $\sigma_{\text{crystal}}/\sigma_{\text{solution}}=55$  at  $2h\nu=28\,800\text{ cm}^{-1}$ . This result is somewhat higher than that previously reported.<sup>25,26</sup>

### C. The Solution Data

The cross sections for two-photon absorption for anthracene in benzene solution were measured at room temperature at four energies. Plots of  $F$  vs  $I$  revealing again the expected  $I^2$  dependence are presented in Fig. 5. The absolute values of the cross sections were calculated using the result of Sec. III.B and are displayed in Fig. 6. From these results we conclude that:

(a) As in the case of the crystal spectrum only a very weak two-photon absorption is observed 26 000–

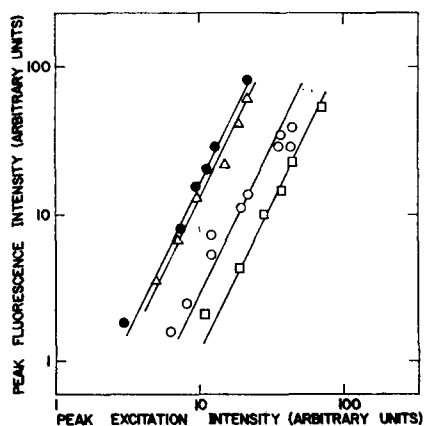


FIG. 5. The dependence of the two-photon-excited peak fluorescence intensity in a 0.09M solution of anthracene in benzene on the peak excitation intensity.  $\Delta$   $2h\nu=28\,800\text{ cm}^{-1}$ ,  $\bullet$   $2h\nu=27\,488\text{ cm}^{-1}$ ,  $\circ$   $2h\nu=26\,820\text{ cm}^{-1}$ ,  $\square$   $2h\nu=26\,112\text{ cm}^{-1}$ . All the  $F$  and  $I$  data are displayed on the same arbitrary scale.

26 800  $\text{cm}^{-1}$  which corresponds to the 0-0 line in one-photon absorption to the  ${}^1B_{2u}$  state.

(b) There is a tenfold increase in  $\sigma$  with increasing energy in the region 26 800–27 500  $\text{cm}^{-1}$ .

(c) Unlike the crystal spectrum no further increase of  $\sigma$  at higher energies is observed. The cross sections at  $2h\nu=27\,488\text{ cm}^{-1}$  and at  $2h\nu=28\,800\text{ cm}^{-1}$  are found to be equal within the limit of error.

## IV. DISCUSSION

In the experiment reported herein we have measured the two-photon spectrum of crystalline anthracene and of the anthracene molecule in the energy range 24 800–28 800  $\text{cm}^{-1}$ . In Fig. 7 we have compiled all the available experimental data for this system. We shall now turn our attention to the theory of two-photon-absorption processes, which will be then applied for a semiquantitative interpretation of our experimental data.

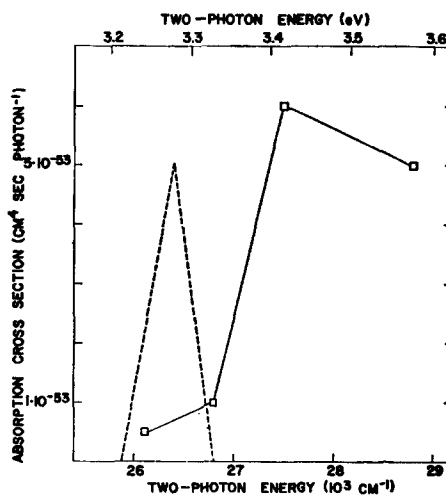


FIG. 6. The energy dependence of the two-photon-absorption cross sections of anthracene in benzene solution. The dashed triangle represents the one-photon-excited 0-0 line corresponding to the  ${}^1A_{1g} \rightarrow {}^1B_{2u}$  transition (see Ref. 36).

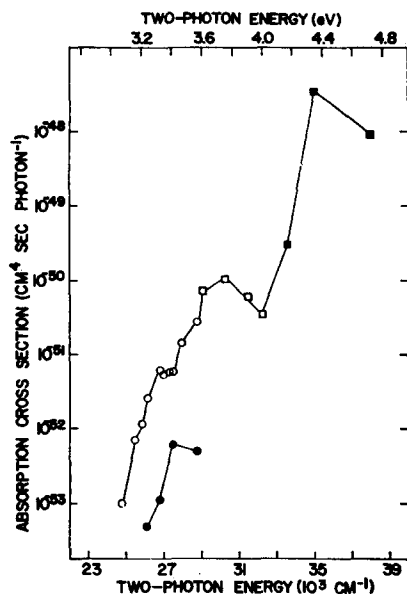


FIG. 7. Summary of the available experimental data on the energy dependence of two-photon absorption in anthracene.  $\blacksquare$ , Storme's crystal data (Ref. 24);  $\square$ , Fröhlich and Mahr's crystal data for  $b$  polarization (Ref. 23) converted for the absorption of two photons of equal energies;  $\circ$ , crystal data from present work;  $\bullet$ , solution data from present work. In the work of Fröhlich and Mahr (Ref. 23), the energy of one photon from the Nd laser is 1.15 eV. For two-photon energy  $E$ , the energy of the second photon is  $E_p=(E-1.15)$  eV. Assuming that the  ${}^1B_{2u}$  state at 3.15 eV acts as the main intermediate virtual state in the two-photon absorption, the cross sections reported by Fröhlich and Mahr are now multiplied by the correction factor

$$\left[ \frac{(3.15 - E_p)}{(3.15 - \frac{1}{2}E)} \right]^2 \left( \frac{E}{2E_p} \right).$$

### A. Brief Theoretical Survey

The usual theoretical scheme underlying the treatment of two-photon transitions was based in the calculation of the total integrated two photon absorption cross sections.<sup>1,38,39</sup> In order to gain a better understanding of the nonlinear optical effects in molecules and in molecular crystals of polyatomic molecules it will be useful to consider transitions between vibronic levels.<sup>39</sup> The two-photon-transition probability between the vibronic states  $gi$  and  $fj$  (where  $g$  and  $f$  correspond to the ground and the final excited electronic states while  $i$  and  $j$  represent vibronic components in these states) is given by<sup>39,40,47</sup>

$$\sigma = \alpha_f g(\nu_\mu) \nu_\lambda \nu_\mu |S_{gi,fj}|^2, \quad (2)$$

where  $\nu_\lambda$  and  $\nu_\mu$  correspond to the angular frequencies of the two absorbed photons,  $\alpha_f$  is the fine-structure constant,  $g(\nu_\mu)$  is the line-shape function, and  $S_{gi,fj}$  is the transition matrix element determined by the interaction Hamiltonian  $H_{\text{int}} = -(e/mc)\mathbf{p} \cdot \mathbf{A} + (e^2/2mc^2)A^2$ . In the dipole approximation one gets the Goepfert-Mayer sum:

$$S_{gi,fj} = \sum_k \sum_l \left[ \frac{\langle gi | M^\lambda | kl \rangle \langle kl | M^\mu | fj \rangle}{\Delta_{gi,kl}^\lambda} + \frac{\langle gi | M^\mu | kl \rangle \langle kl | M^\lambda | fj \rangle}{\Delta_{gi,kl}^\mu} \right], \quad (3)$$

where  $M^\lambda = \mathbf{e}_\lambda \cdot \mathbf{M}$ , with  $\mathbf{e}_\lambda$  corresponding to the polarization vector of the photon  $\nu_\lambda$  and  $\mathbf{M}$  is the transition dipole-moment operator, while

$$\Delta_{gi,kl}^\lambda = \hbar^{-1}(E_{gi} + \hbar\nu_\lambda - E_{kl})$$

corresponds to the energy denominator between the vibronic states. The double sum involves all the intermediate  $kl$  vibronic states. Application of the following approximations<sup>39</sup> leads to considerable simplifications:

(a) The energy denominators for an off-resonance case can be taken as determined by the electronic energy gap so that  $\Delta_{gi,kl}^\lambda = \Delta_{gk}^\lambda$ .

(b) First-order vibronic-coupling Herzberg-Teller perturbation theory can be applied considering level mixing by intramolecular vibronic terms which are linear in the nuclear displacements.<sup>48</sup>

(c) Approximate quantum-mechanical sum rules for the vibrational functions:  $\sum_l |l\rangle \langle l| = 1$ , do apply.<sup>48,49</sup> Under these circumstances the two-photon-transition matrix element can be displayed in the form<sup>39,50</sup>:

$$S_{gi,fj} = \alpha \langle i | j \rangle + \sum_a (\beta_a + \gamma_a) \langle i | q_a | j \rangle. \quad (4)$$

<sup>47</sup> B. Honig and J. Jortner, J. Chem. Phys. **47**, 3698 (1967).

<sup>48</sup> A. C. Albrecht, J. Chem. Phys. **33**, 156, 169 (1959).

<sup>49</sup> A. C. Albrecht, J. Chem. Phys. **34**, 1476 (1961).

<sup>50</sup> Application of coordinate-momentum commutation relations (see Ref. 47) led to simplification of the results presented in Ref. 39.

The first term in Eq. (4) corresponds to a symmetry-allowed transition

$$\alpha = \sum_{k^0} [\langle g^0 | m^\lambda(g, k) | k^0 \rangle \langle k^0 | M^\mu | f^0 \rangle + \langle g^0 | m^\mu(g, k) | k^0 \rangle \langle k^0 | M^\lambda | f^0 \rangle], \quad (5)$$

with  $m^\lambda(g, k) = M^\lambda / \Delta_{gk}^\lambda$ . The matrix element  $\langle i | j \rangle$  involves the customary vibrational overlap Franck-Condon factor which partitions the total intensity among the vibronic components. The states  $g^0$ ,  $k^0$ , and  $f^0$  correspond to the zero-order (harmonic) electronic states. The second contribution to Eq. (4) involves the symmetry-forbidden pathways. The terms  $\beta_a$  correspond to the case where upon the transition  $g^0 \rightarrow k^0$  is allowed while the transition  $k^0 \rightarrow f^0$  is symmetry forbidden, while the terms  $\gamma_a$  represent the case when  $g^0 \rightarrow k^0$  is forbidden while  $k^0 \rightarrow f^0$  is allowed. These are given in the form:

$$\beta_a = \sum_{k^0} \sum_{p^0} [\langle g^0 | m^\lambda(g, k) | k^0 \rangle \langle k^0 | M^\mu | p^0 \rangle \Lambda_a(p^0, f^0) + \langle g^0 | m^\mu(g, k) | k^0 \rangle \langle k^0 | M^\lambda | p^0 \rangle \Lambda_a(p^0, f^0) + \langle g^0 | m^\lambda(g, k) | k^0 \rangle \Lambda_a(k^0, p^0) \langle p^0 | M^\mu | f^0 \rangle + \langle g^0 | m^\mu(g, k) | k^0 \rangle \Lambda_a(k^0, p^0) \langle p^0 | M^\lambda | f^0 \rangle], \quad (5a)$$

$$\gamma_a = \sum_{k^0} \sum_{s^0} [\langle g^0 | m^\lambda(g, k) | s^0 \rangle \Lambda_a(s^0, k^0) \langle k^0 | M^\mu | f^0 \rangle + \langle g^0 | m^\mu(g, k) | s^0 \rangle \Lambda_a(s^0, k^0) \langle k^0 | M^\lambda | f^0 \rangle + \Lambda_a(g^0, s^0) \langle s^0 | m^\lambda(g, k) | k^0 \rangle \langle k^0 | M^\mu | f^0 \rangle + \Lambda_a(g^0, s^0) \langle s^0 | m^\mu(g, k) | k^0 \rangle \langle k^0 | M^\lambda | f^0 \rangle]. \quad (5b)$$

The vibronic coupling mixing coefficients for the scrambling of the initial ( $g^0$ ) intermediate ( $k^0$ ) and final ( $f^0$ ) zero-order states with the (harmonic) states  $s^0$  on  $p^0$  are given in the simple form<sup>39,48,49</sup>:

$$\Lambda_a(u^0, v^0) = (E_{v^0} - E_{u^0})^{-1} \langle u^0 | \partial H_M / \partial q_a | v^0 \rangle \quad (6)$$

for any pair of electronic functions  $u^0$  and  $v^0$ . The set  $\{q_a\}$  corresponds to the normal coordinates of the system and  $H_M$  is the molecular Hamiltonian. From these results we conclude that:

(a) For symmetry-allowed two-photon transitions (when  $\alpha \neq 0$ ) the  $\beta_a$  and  $\gamma_a$  terms, (for all  $q_a$ ) are negligible in most cases. The vibrational structure of the even-parity spectrum will be determined by the ordinary vibrational overlap integrals.

(b) In the case of a symmetry-forbidden two-photon transition (when  $\alpha = 0$ ) the vibrations inducing mixing of states have to be characterized by the proper symmetry so that the matrix elements appearing in Eq. (6) will be nonvanishing for some vibrational modes  $q_a$ .

(c) The vibrational structure of the symmetry-

forbidden two-photon transitions is determined by the vibrational integrals  $\langle i | q_a | j \rangle$  as is evident from Eq. (4). Thus, as in the case of vibronically-induced one-photon transitions,<sup>48</sup> the 0-0 line is missing and the two-photon spectrum will consist of a totally symmetric progression built on a false origin.<sup>39</sup> In this case the vibrational structure of the two-photon  $g \rightarrow u$  forbidden transition will differ from the one-photon allowed pathway, as a false origin will appear in the case of the two-photon transition, being blue shifted from the true origin which corresponds to the one-photon transition. This energy shift will be equal to the frequency of the vibration which dominates the vibronic coupling. It can, however, happen that several vibrations are responsible for vibronic coupling in the ground, intermediate, and final states, so that several false origins will appear in this case. We should note in passing that the vibronic coupling in the ground state is usually small (due to a large energy denominator) and that the vibronic coupling in the final state seems to be more important than that in the intermediate virtual states.<sup>39b</sup>

(d) A supporting evidence for the assignment of symmetry-allowed and symmetry-forbidden two-photon transitions can be derived from the absolute cross sections. Semiempirical calculations<sup>38-40</sup> led to the value of  $\sigma \sim 10^{-48}$  cm<sup>4</sup>·sec photon<sup>-1</sup> for allowed transitions in aromatic molecules. Calculations on symmetry-forbidden transitions in benzene<sup>39</sup> led to the value of  $\sigma \sim 10^{-51}$ - $10^{-52}$  cm<sup>4</sup>·sec photon<sup>-1</sup> in this case. Finally we should note that symmetry-forbidden transitions can be induced by quadrupole contributions arising both from the  $A^2$  interaction term in first order and from the second order (quadrupole) contribution to the  $\mathbf{p} \cdot \mathbf{A}$  term. Previous estimates by Honig *et al.*<sup>39</sup> led to the conclusion that the contribution of the quadrupole term should lead to a two-photon cross section of the order of  $10^{-53}$ - $10^{-54}$  cm<sup>4</sup>·sec photon<sup>-1</sup>. For the case of symmetry-forbidden two-photon transition, the quadrupole induced transition differs in one important aspect from the vibronically induced transition, as the vibrational structure expected for the former case will just reproduce the features of the one-photon transition, and will be built on the true electronic origin. Finally we should point out that the order-of-magnitude estimates presented herein for the  $\sigma$  values of aromatic molecules should be also valid for Frenkel exciton states in molecular crystals.

### B. A Vibronically Induced Two-Photon Transition

The two-photon excited state in crystalline anthracene observed in the region 26 000-27 500 cm<sup>-1</sup> is assigned to the symmetry-forbidden  ${}^1A_{1g} \rightarrow {}^1B_{2u}$  two-photon transition because of the following reasons:

(a) The observation of a false vibrational origin: The mean value of the one-photon active-crystal Davydov

components for the  ${}^1A_{1g} \rightarrow {}^1B_{2u}$  0-0 band is located at 25 320 cm<sup>-1</sup>. The first peak of the two-photon transition is located in the region 26 400-26 750 cm<sup>-1</sup> (Figs. 3 and 7). Hence the two-photon transition is blue shifted relative to the corresponding one-photon state by  $1300 \pm 400$  cm<sup>-1</sup>. This situation corresponds to a vibronically induced two-photon transition.

(b) The absolute intensity: The intensity of this transition  $\sigma \sim 5 \times 10^{-52}$  cm<sup>4</sup>·sec photon<sup>-1</sup> in the crystal is consistent with the order-of-magnitude estimates for a symmetry-forbidden transition.

Turning now our attention to the solution spectra we assign the state in the range 26 800-28 800 cm<sup>-1</sup> (Fig. 6) to the  ${}^1A_{1g} \rightarrow {}^1B_{2u}$  symmetry-forbidden transition. The blue shift of the two-photon transition relative to the 0-0  ${}^1B_{2u}$  one-photon state in solution is  $1100 \pm 400$  cm<sup>-1</sup>. The  $\sigma$  value for this two-photon transition is again consistent with the value for a vibronically induced transition.

The following features of the  ${}^1A_{1g} \rightarrow {}^1B_{2u}$  two-photon transition observed both in the crystal and in the single molecule should be now compared:

(a) The nontotally symmetric vibration inducing the two-photon transition both in the crystal and in solution is characterized by the frequency  $1200 \pm 400$  cm<sup>-1</sup> (where a near value has been taken). This result provides another strong support to our assignment of this transition. Provided that vibronic coupling in the final ( $f^0$ ) state is dominant we then expect that vibrations of the symmetry  $b_{2u}$  and  $b_{3u}$  couple the  ${}^1B_{2u}$  state with  ${}^1A_{1g}$  and  ${}^1B_{1g}$  states. The corresponding vibrational frequencies of appropriate symmetry, which involve skeleton deformation and ring stretching are: 615 cm<sup>-1</sup> ( $b_{3u}$ ), 1398 cm<sup>-1</sup> ( $b_{3u}$ ), 1462 cm<sup>-1</sup> ( $b_{3u}$ ), 1533 cm<sup>-1</sup> ( $b_{3u}$ ), 743 cm<sup>-1</sup> ( $b_{2u}$ ), 907 cm<sup>-1</sup> ( $b_{2u}$ ), 1316 cm<sup>-1</sup> ( $b_{2u}$ ), 1448 cm<sup>-1</sup> ( $b_{2u}$ ), and 1620 cm<sup>-1</sup> ( $b_{2u}$ ).<sup>51</sup> One (or more) of these vibrations may be active in inducing this symmetry-forbidden two-photon transition. To ascertain the role of individual vibrations in the intramolecular coupling, high-resolution two-photon spectra are required.

(b) The crystal to solution spectral shift for this two-photon transition is found to be  $-700 \pm 200$  cm<sup>-1</sup> (see Fig. 7). This result is in good agreement with the corresponding ( $-700$  cm<sup>-1</sup>) crystal to the benzene solution spectral shift reported for the  ${}^1A_{1g} \rightarrow {}^1B_{2u}$  one-photon transition.<sup>36b</sup>

(c) The cross sections for the symmetry-forbidden two-photon transitions in the crystal and in the single molecule differ by about one order of magnitude (Fig. 7),  $\sigma_{\text{crystal}}/\sigma_{\text{molecule}} \sim 10$ . This result is reliable within a numerical factor of 2. The enhancement of the two-photon transition in the crystal is reasonable in

<sup>51</sup> S. Califano, J. Chem. Phys. **36**, 903 (1962).



view of the available data on single-photon spectroscopy in this system.<sup>36a,52</sup> The total oscillator strength for the one-photon transition to the Davydov components of the  ${}^1B_{2u}$  state in the crystal was reported to be higher by a factor of 4 than the oscillator strength for the corresponding  ${}^1A_{1g} \rightarrow {}^1B_{2u}$  transition in solution.<sup>36a,52</sup> This hypochromic effect can be partially rationalized in terms of crystal field mixing between the  ${}^1B_{2u}$  and the intense  ${}^1B_{3u}$  state (and other excited  $u$ -type  $\pi \rightarrow \pi^*$  transitions) in the crystal. The theoretical calculations of Silbey *et al.*<sup>53</sup> indicate that the oscillator strength should increase by about a factor of 1.5–2.0 in the crystal relative to the free-molecule value, in rough agreement with Brodin's results. It should be stressed that both the experimental one-photon  $f$  values and our values do not contain a proper correction to inner field effects so that a detailed quantitative comparison of one- and two-photon-absorption cross sections with theory cannot be yet performed.

To elucidate the role of crystal-field mixing effect in our case, we should notice that in the rigid crystal configuration interaction can be induced only between states of the same symmetry so that matrix elements between  $g$  and  $u$  crystal states, such as  $\langle A_u | H_c | A_g \rangle$  vanish. Crystal-field mixing does not occur between the  ${}^1B_{2u}$  state and the  ${}^1A_{1g}$  or the  ${}^1B_{1g}$  states. However, crystal-field mixing in the intermediate  $u$ -type states may lead to the observed intensity enhancement in the crystal cross sections relative to the single molecule values.

(d) The meager information obtained by us concerning the vibrational structure of this two-photon transition should be considered. The vibrational Franck–Condon integrals obtained for the  $A_{1g}(0) \rightarrow {}^1B_{1u}(v)$  single-photon transition (where  $v=0, 1, \dots$  corresponds to the vibrational quantum member of the  $a_{1g}$  vibration), are<sup>36</sup>  $|\langle 0 | 0 \rangle|^2 = 0.32$ ,  $|\langle 0 | 1 \rangle|^2 = 0.31$ , and  $|\langle 0 | 2 \rangle|^2 = 0.22$ . Thus, provided that in the solution spectrum the two-photon false origin is located at  $27\,200\text{ cm}^{-1}$ , then the solution absorption at  $28\,800\text{ cm}^{-1}$  corresponds to the first component of the totally symmetric  $a_{1g}$  progression, characterized by frequency spacing of  $1410\text{ cm}^{-1}$ .<sup>36b</sup> The observed cross sections at these energies are consistent with the Franck–Condon factors for this progression.<sup>53</sup> Assuming that the false two-photon origin in the crystal is located at about  $26\,600\text{ cm}^{-1}$ , we cannot assign the steeply increasing two-photon absorption at energies higher than  $27\,500\text{ cm}^{-1}$  to a vibrational component of the same transition, as these cross sections are inconsistent with the appropriate vibrational overlap factors. From the comparison of the solution and the crystal spectra (Fig. 7) we can conclude that a new state is observed in the

even-parity spectrum of the crystal which does not appear in the solution spectrum.

### C. Two-Photon Allowed Transitions

The large two-photon-absorption cross sections observed by Storme<sup>24</sup> in the range 4.2–4.8 eV are assigned to the symmetry-allowed  ${}^1A_{1g} \rightarrow {}^1B_{1g}$  and  ${}^1A_{1g} \rightarrow {}^1A_{1g}$  transitions. This assignment is consistent with the theoretical molecular calculations of Pariser<sup>33</sup> which predicted that these molecular states should be located at 4.9 eV. The absorption cross sections in this region  $\sigma \sim 10^{-48}\text{ cm}^4 \cdot \text{sec photon}^{-1}$  are consistent with the assignment of an allowed even-parity transition.

As previously pointed out, the exciton states located above 4.1 eV in crystalline anthracene are metastable.<sup>35</sup> However, the dominating decay channel involves an intramolecular radiationless decay process. The study of Bixon and Jortner<sup>54</sup> demonstrates that in this case inhomogeneous line broadening will occur, while the integrated intensity of these transitions will be not affected. Hence, it is justified<sup>35</sup> to use the molecular states to estimate the two-photon-absorption cross sections (or the one-photon  $f$  numbers) for metastable exciton states in these molecular crystals.

It is interesting to speculate on the relative location of the  ${}^1A_{1g}$  and  ${}^1B_{1g}$  states in the single molecule and in the crystal. In their attempt to elucidate the nature of the crystal state located at 3.5–3.6 eV (Fig. 7), Hernandez and Gold<sup>27</sup> argued that the  ${}^1A_g$  and  ${}^1B_g$  crystal exciton states originating from the  ${}^1B_{1g}$  molecular state are red shifted in the crystal by about  $-1.4\text{ eV}$ . The energies,  $E_i$ , of even- and odd-parity exciton states are given by the Davydov's formula<sup>28,36b,53</sup>

$$E_i = \Delta e^f + D^f + I_{\text{eq}}(\mathbf{k}=0) + I_i(\mathbf{k}=0), \quad (7)$$

where the index  $i=1, 2$  corresponds to the two branches of the exciton band (for this monoclinic crystal characterized by two molecules per unit cell),  $\Delta e^f$  is the gas-phase excitation energy,  $D^f$  is the uniform medium shift (independent of the exciton momentum  $\mathbf{k}$ ), arising from first-order intermolecular interactions and from second-order dispersion forces.  $I_{\text{eq}}(\mathbf{k}=0)$  corresponds to the excitation transfer terms between translationally equivalent molecules, while  $I_i(\mathbf{k}=0)$  represents a linear combination of the interaction terms between the reference molecule and the translationally inequivalent molecules. We have to set  $\mathbf{k} \sim 0$ , as two-photon transitions to exciton states are expected to obey the same  $\mathbf{k}$  selection rule as for one-photon states (i.e.,  $\mathbf{k}=\mathbf{Q}$ , where  $\mathbf{Q}$  is the wave vector of the exciting light), as momentum is conserved in virtual transitions. The crystal shift of the center of gravity of the Davydov components, relative to the gas-phase spectrum, is just  $D^f + I_{\text{eq}}(\mathbf{k}=0)$ . Hernandez and Gold<sup>27</sup> have con-

<sup>52</sup> M. S. Brodin and S. V. Marisova, *Opt. Spectrosc.* **19**, 132 (1965).

<sup>53</sup> R. Silbey, J. Jortner, and S. A. Rice, *J. Chem. Phys.* **42**, 1515 (1965).

<sup>54</sup> M. Bixon and J. Jortner, *J. Chem. Phys.* **48**, 715 (1968).

cluded that for the  ${}^1B_{1g}$  crystal state  $I_{\text{eq}}(\mathbf{k}=0) = 0.1$  eV while  $D^f = -1.3$  eV, the major contribution to the latter term arising from dispersion forces. This result is somewhat surprising, as on qualitative grounds the  $D^f$  term should not exceed the heat of sublimation of the crystal. Indeed, for the  ${}^1B_{2u}$ -type state analysis of the available experimental data<sup>36b</sup> leads to  $D^f = -1500$   $\text{cm}^{-1}$ . Our objections to the assignment of Hernandez and Gold rest on the following arguments:

(a) From the theoretical point of view the estimate of the dispersion contribution is unreliable as it rests on a closure (mean energy) approximation for a second-order perturbation expansion.

(b) From the experimental point of view we notice that the two-photon-absorption cross sections at 3.5–3.6 eV are by two orders of magnitudes lower than the  $\sigma$  values observed in the region 4.2–4.7 eV (which correspond to symmetry-allowed transitions to Frenkel exciton states). It is thus unlikely that the 3.5–3.6-eV state corresponds to a crystal-shifted symmetry-allowed two-photon transition to a Frenkel state.

#### D. The Anthracene Crystal State at 3.5–3.6 eV

The increase of the two-photon-absorption cross sections in crystalline anthracene in the energy range above 27 500  $\text{cm}^{-1}$  has no counterpart in the solution spectrum of the single molecule. Our results combined with the previous data of Fröhlich and Mahr<sup>23</sup> clearly demonstrate the existence of a two-photon excited crystal state in this energy region characterized by  $\sigma \sim 5 \times 10^{-51}$   $\text{cm}^4 \cdot \text{sec photon}^{-1}$ . Guided by the arguments presented above, it is unlikely to assign this state to a  ${}^1A_{1g} \rightarrow {}^1B_{1g}$  transition. Another attractive possibility was offered by Albrecht<sup>41</sup> who assigned this state to the symmetry-forbidden  ${}^1A_{1g} \rightarrow {}^1B_{3u}^-$  transition, as according to theoretical calculations<sup>37</sup> the  ${}^1B_{3u}^-$  state is located at 3.7 eV. Evidence against this assignment is provided by the marked difference between the crystal and the solution spectra. As we have pointed out before, the crystal shift for a Frenkel state is  $D^f + I_{\text{eq}}$ . Denoting by  $W^f$  the corresponding solvent shift in benzene solution, the crystal-solution shift is  $\delta = D^f + I_{\text{eq}} - W^f$ . In the case of the  ${}^1B_{2u}$  ( $p$ -type) state of anthracene,  $I_{\text{eq}} = -700 \pm 200$   $\text{cm}^{-1}$ ,<sup>36b</sup> so that the major contribution to the crystal-solution spectral shift  $\delta = -700$   $\text{cm}^{-1}$  arises from the exciton term  $I_{\text{eq}}$ , while the “solvent” shifts are about equal in the two cases, i.e.,  $W^f \sim D^f$ . In the case of the  $B_{3u}^-$  ( $\alpha$ -type) excited states of aromatic molecules, the intermolecular excitation exchange interactions are dominated by short-range interactions,<sup>23,36b,42</sup> unlike in the  ${}^1B_{2u}$  state where long-range dipole-dipole interactions prevail. Exciton states arising from the  $\alpha$ -type excited state in crystalline benzene and naphthalene are characterized by a very small  $I_{\text{eq}}$  term,<sup>42</sup> e.g.,  $I_{\text{eq}} \approx 0 \pm 10$   $\text{cm}^{-1}$ . As we expect that  $W^f \sim D^f$  for the  ${}^1B_{3u}^-$

state of anthracene, the shift  $\delta$  will be small for this state. Therefore it cannot be argued that the  ${}^1B_{3u}^-$  state should be appreciably red shifted in crystalline anthracene relative to the solution spectrum. This argument combined with the experimental results provide strong circumstantial evidence against the assignment of the crystal state to the symmetry-forbidden  ${}^1A_{1g} \rightarrow {}^1B_{3u}^-$  transition.

We propose an alternative assignment and tentatively identify the state at 3.5–3.6 eV as corresponding to crystal states which have no analog in the free molecule. It is proposed that this state corresponds to a  $g$ -type charge-transfer state of the crystal. This assignment is consistent with the following observations:

(a) The location of this crystal state is consistent with the experimental evidence of Pope and Burgos,<sup>30</sup> who on the basis of their electron-emission experiments proposed that a charge-transfer state is located at 3.45 eV in crystalline anthracene.

(b) The magnitude of the two-photon-absorption cross section is consistent with this assignment. The oscillator strength for the one-photon absorption to a  $u$ -type crystal state is expected to be rather low. Early estimates<sup>43</sup> based on intermolecular overlap considerations led to the value of  $f \sim 10^{-4} - 10^{-5}$ .<sup>43</sup> Applying Mulliken's ideas<sup>56</sup> to crystal charge-transfer states it is conceivable that the major source of intensity for odd-parity one-photon excitations of these states will result from configuration interaction between charge-transfer and Frenkel exciton states.<sup>56</sup> An oscillator strength of the order  $f \sim 10^{-3} - 10^{-2}$  seems reasonable. We thus expect that the two-photon-absorption cross sections for the symmetry-allowed two-photon excitation to the  $g$ -type charge-transfer state will be about  $\sim 1\%$  of the cross section for the symmetry-allowed  ${}^1A_{1g} \rightarrow {}^1B_{1g}$ ,  $A_{1g}$  two-photon transitions to Frenkel states, i.e.,  $\sigma \sim 10^{-50} - 10^{-51}$   $\text{cm}^4 \cdot \text{sec photon}^{-1}$ . This rough estimate is consistent with the experimental results.

This assignment of charge-transfer states deserve further experimental and theoretical study. From the experimental point of view, two-photon spectroscopy should lead to the location of charge-transfer states in the tetracene crystal (at 2.9 eV<sup>57</sup>) and in the naphthalene crystal (at about 4.4 eV<sup>29</sup>). From the theoretical point of view studies of the two-photon even-parity transitions to  $g$ -type charge-transfer states will be of considerable interest.

#### E. The Low-Energy Two-Photon Absorption

Finally we turn our attention to the very low two-photon-absorption cross sections observed both in the

<sup>55</sup> R. S. Mulliken and W. B. Pearson, *Ann. Rev. Phys. Chem.* **13**, 107 (1962).

<sup>56</sup> S. I. Choi (private communication).

<sup>57</sup> N. Geacintov and M. Pope, *J. Chem. Phys.* **45**, 3884 (1966).

crystal and in solution in the range of the zeroth vibronic component of the  ${}^1B_{2u}$  state (24 800–26 000  $\text{cm}^{-1}$  in the crystal and 26 000–26 800  $\text{cm}^{-1}$  in solution). On the basis of the crystal data this absorption does not arise from hot bands. It is conjectured that this weak absorption may be due to quadrupole contributions arising both from the  $A^2$  and the  $\mathbf{p}\cdot\mathbf{A}$  term in the interaction Hamiltonian.<sup>39</sup> The order-of-magnitude estimate<sup>39</sup> of the quadrupole two-photon transition given above  $\sigma\sim 10^{-53}\text{--}10^{-54}\text{ cm}^4\cdot\text{sec photon}^{-1}$  is consistent with the experimentally observed cross sections in this range. The contribution of the  $A^2$  term to  $\sigma$  in this region may be established by excitation with circularly polarized light, whereupon this contribution

of the  $A^2$  term is expected to vanish. It should be pointed out that this assignment is by no means certain as considerable experimental difficulties are involved in the determination of these very low two-photon cross sections.

#### ACKNOWLEDGMENTS

We wish to thank M. Levine for his technical assistance and B. Honig for helpful discussions.

This research was partially supported by the Air Force Office of Scientific Research. We have also benefited from the use of facilities provided by the Advanced Research Projects Agency for materials research at the University of Chicago.

### Cotton–Mouton Effect through an Absorption Band

A. C. BOCCARA, J. FERRE, B. BRIAT, M. BILLARDON, AND J. P. BADOZ

*Ecole de Physique et de Chimie Industrielles,\* 10 rue Vauquelin, Paris, France*

(Received 9 August 1968)

Cotton–Mouton dichroism was measured for an aqueous solution of europium trichloride. The experiment was performed at room temperature through the visible  ${}^7F_6\rightarrow{}^5D_1$  absorption band. A phenomenological theory is given for the results thus obtained. The spectroscopic splitting factor of the excited state is determined and is shown to be in close agreement with that obtained independently through Faraday effect measurements. Optimal experimental conditions are pointed out for further work in the field.

#### INTRODUCTION

Recently there has been a great resurgence of interest<sup>1,2</sup> in magnetically induced optical activity (the so-called Faraday effect). The phenomenon is observable in all substances submitted to a magnetic field  $H$  coincident with the direction of propagation of a beam of polarized light. As with natural optical activity, one observes "anomalous" magnetic optical rotatory dispersion (MORD) as well as magnetic circular dichroism (MCD) when measurements are performed through absorption bands. The data thus obtained are of great interest to spectroscopists and chemists. On the other hand, it is fair to say that the Cotton–Mouton effect<sup>3,4</sup> predicted when  $H$  is applied perpendicular to the light beam, has not been the object of much attention. This can be readily understood since the phenomenon is

small and requires a very sensitive apparatus to be detected. In the Cotton–Mouton configuration, there exists an absorption difference for light polarized either parallel or perpendicular to the magnetic field. This is referred to as the Cotton–Mouton dichroism. Occurring simultaneously is a difference in the indices of refraction  $\Delta n = n_{\perp} - n_{\parallel}$  (the Cotton–Mouton birefringence). Recent work in the field is largely due to Suits, Argyle, and their co-workers<sup>5–7</sup> who considered material containing dipositive europium. Their measurements were restricted to the red edge of the strong visible absorption bands. In a recent article,<sup>8</sup> Bogaard *et al.* made some predictions for the Cotton–Mouton effect in atomic sodium and lithium.

The aim of this paper is to report on an original experiment concerning Cotton–Mouton dichroism. Measurements were performed through the entire range of an electronic absorption band at room tem-

\* Equipe CNRS du Laboratoire d'Optique Physique.

<sup>1</sup> See, for example, (a) A. D. Buckingham and P. J. Stephens, *Ann. Rev. Phys. Chem.* **17**, 399 (1966); (b) A. J. McCaffery, P. J. Stephens, and P. N. Schatz, *Inorg. Chem.* **6**, 1614 (1967).

<sup>2</sup> B. Briat and C. Djerassi, *Nature* **217**, 918 (1968).

<sup>3</sup> See for example, A. Cotton and H. Mouton, *Ann. Chim. Phys.* **11**, 145, 289 (1907).

<sup>4</sup> See J. W. Beams, *Rev. Mod. Phys.* **4**, 133 (1932), for further references.

<sup>5</sup> J. C. Suits, B. E. Argyle, and M. J. Freiser, *J. Appl. Phys.* **37**, 1396 (1966).

<sup>6</sup> J. C. Suits and B. E. Argyle, *J. Appl. Phys.* **36**, 1251 (1965).

<sup>7</sup> B. E. Argyle, J. C. Suits, and M. J. Freiser, *Phys. Rev. Letters* **15**, 822 (1965).

<sup>8</sup> M. P. Bogaard, A. D. Buckingham, and B. J. Orr, *Mol. Phys.* **13**, 533 (1967).